ADVANCED FUNCTIONAL MATERIALS
www.afm-journal.de

Sol–Gel Synthesis of High-Density Zeolitic Imidazolate Framework Monoliths via Ligand Assisted Methods: Exceptional Porosity, Hydrophobicity, and Applications in Vapor Adsorption

*Elwin Hunter-Sellars, Paola A. Saenz-Cavazos, Anthony R. Houghton, Sean R. McIntyre, Ivan P. Parkin, and Daryl R. Williams**

Monolithic ZIF-8 and ZIF-67 adsorbents are synthesized at room temperature using a novel, ligand-assisted method. Despite reductions in crystallinity within some of the samples, monolithic zeolitic imidazolate frameworks (ZIFs) have superior volume-relative microporosity, total porosity, and surface areas relative to their particulate counterparts due to increased density. Samples synthesized using a single modulator, *n*-butylamine, have a hierarchical porosity resulting in improved adsorption capacities in mid- to high- sorbate pressure regions. ZIF-67 monoliths produced through mixed-modulator synthesis, *n*-butylamine and 1-methylimidazole, are almost entirely microporous. Vapor adsorption isotherms find that, whilst their amorphous content results in increased water uptake, monolithic ZIFs are found to possess higher surface and adsorption hydrophobicity than traditional non-polar adsorbents. Cosorption measurements with a common VOC toluene, under humid conditions, find that these monolithic ZIF samples outperform powder equivalents, with the mixed-modulator ZIF-67 monolith capturing 28% more VOC compared to the powder ZIFs studied due to its superior volumetric efficiency. This study provides insights into the benefits of modulator-based tuning of porosity within monolithic ZIFs which, combined with their hydrophobicity, may facilitate their application for industrial organic vapor recovery or indoor air cleaning, where efficient hydrophobic adsorbents which can operate in humid environments are essential.

1. Introduction

Zeolitic imidazolate frameworks (ZIFs), are a class of metal-organic-frameworks (MOFs) consisting of metal ions (commonly zinc[1]) connected by imidazole linkers. The angle of 145° formed by the metal centers and linker molecules is analogous to the bridging angle of Si—O—Si bonds in zeolites, giving ZIFs a zeolite-like topology.[1–3] ZIFs are commonly utilized as adsorbents due to their high surface area and the ability to tune their pore size and properties based on the metal ion and imidazole linker species used,[1,3] with several dozen topologies and over a hundred unique structures for ZIFs existing.[1,4] ZIF-8 and ZIF-67 are formed by the reaction of 2-methylimidazole with zinc and cobalt salts, respectively, and both possess sodalite-like topology, with two apertures of sizes 3.4 and 11.6 Å.[5] Studies on ZIF-8 powders have found the materials are suitable adsorbents for several applications including vapor phase hydrocarbon capture[6–8] and liquid-phase contaminant extraction.[9,10] Due to the hydrophobicity of the 2-methylimidazole linker, ZIF-8 has been found to have low affinity toward water vapor,[6,11] making it particularly suitable for adsorption applications where humidity's competition for adsorption sites plays a key role,[12,13] such as indoor air cleaning of volatile organic compounds (VOCs).[14–16] ZIF-67 has been found to be unstable in liquid water, with a noted loss in crystallinity,[17] and water vapor isotherms of the material have not been reported in the literature.

Whilst many particulate adsorbents possess good molecular adsorption kinetics[18] several operational difficulties exist when integrating fine particulates into adsorption processes including large pressure drops in adsorbent packed columns as well as challenges with adsorbent recovery and recycling. Structured monolithic adsorbents with their intrinsically larger and better defined physical dimensions, have several advantages including greater mechanical stability,[19,20] reduced pressure drop,[19] higher heat transfer,[19] and higher volumetric efficiency.[19–21] The most common methods of creating structured adsorbents is through

E. Hunter-Sellars, P. A. Saenz-Cavazos, A. R. Houghton, S. R. McIntyre, Prof. D. R. Williams
Department of Chemical Engineering
Imperial College London
London SW7 2AZ, UK
E-mail: d.r.williams@imperial.ac.uk
Prof. I. P. Parkin
Department of Chemistry
University College London
London WC1E 6BT, UK
The ORCID identification number(s) for the author(s) of this article can be found under https://doi.org/10.1002/adfm.202008357.

DOI: 10.1002/adfm.202008357

compression of particulate adsorbents, either thermally[22] mechanically,[23] or through the use of binding materials such as clay or alumina.[24] A study on the compaction of UiO-66 based MOFs through hydraulic compaction[23] found that while the increased pressure resulted in some loss of crystallinity, the density of the pellet was found to be almost three times that of the powder, as well as having increased hydrogen gas storage capabilities.

The synthesis of metal-organic frameworks via sol–gel methods has gained traction in recent years,[25,26] due to their ease of production as well as the ability to introduce new pore size regimes into the material.[27] A review by Sumida et al.[28] found studies utilizing sol–gels for chemical functionalization of MOFs, forming MOF-substrate composites, and creating higher-order structures such as thin films and monoliths. Studies on monolithic HKUST-1[26] and UiO-66[27,29] found that the choice of metal source and solvent, as well as the size of the primary particles all affected the formation of a sol–gel. The selection of optimal drying conditions for the gel were also found to be essential, as elevated drying rates may lead to the destruction of the gel's macrostructure and result in a powdered MOF product.[26,27] Several studies report on the synthesis of ZIF monolithic adsorbents, with slowed drying regimes and extended reaction of ZIF-8 crystals being commonly employed. The monoliths reported by Tian[20] and Mehta[21] were found to have lower surface areas than powdered samples, around 1400 $m^2\ g^{-1}$, but improved volumetric efficiency due to their increased density. Gels of ZIF-8 have been prepared through the use of modulating ligands,[30] but the use of these gels for monolith production has not been investigated.

In the current work, the synthesis and characterization of monolithic ZIF-8 and ZIF-67 via ligand-assisted sol–gel formation adsorbents are explored. The methods reported in this study will provide simple, sequential methods for producing monolithic ZIF-8 and ZIF-67 under ambient conditions without the need for high temperature and pressure, or post-synthetic modification. Several synthetic procedures were evaluated in order to test the effect of modulating ligand on the final adsorbent's density, porosity, and volumetric efficiency of gas uptake. The majority of samples were found to have increased density, leading to improvements in the volume-relative porosity when compared to their powder equivalents. The surface chemistry and hydrophobicity of the monoliths was assessed by advancing contact angle measurements and the adsorption of several vapor-phase solvent molecules. The adsorption studies of volatile organic species and water vapor also provides information about the VOC removal potential of monolithic ZIF-8 and ZIF-67, an application of which typically involves high relative humidity and low concentrations of VOCs, as well as other industrial applications where high organic vapor concentrations and humidity are encountered.

2. Results and Discussion

Powder samples of ZIF-8 and ZIF-67 were found to have high crystallinity, matching well with literature reference patterns,[17] as seen in **Figure 1**. ZIF-67 (NB), ZIF-67 (ML), and ZIF-8 (NB) all displayed characteristic peaks at 2θ = 7.4, 10.4, 12.8, 14.8, 16.6, and 18.1, with relative crystallinities of 32.3%, 25.5%, and 21.7%, respectively. The presence of noise and the peak broadening within the diffraction patterns of the monolithic samples is likely due to the presence of amorphous content,[31] with all relative crystallinities for monoliths below 35%. ZIF-8 (ML) was found to be almost entirely amorphous, with peaks only observable at 2θ = 12.8 and 18.1 resulting in a relative crystallinity of <1%. This highly amorphous product may be due to monodentate linkages formed between zinc and cobalt ions and the modulating ligands of *n*-butylamine and 1-methylimidazole.[32] Previous studies on ZIF-8 modulation by *n*-butylamine and 1-methylimidazole separately found distinct crystals could be formed,[30] albeit with a reduced size. The results in this work suggest a mixture of these ligands produces unfavorable conditions for ZIF-8 crystal growth, enough to inhibit any noticeable formation of a crystalline phase. On the other hand, ZIF-67 still appears to be able to form crystalline products successfully even with multiple modulating ligands present.

Figure 2 shows the results of electron microscopy imaging, in which powder samples displayed distinct, well-defined crystals with average diameters of 103 ± 15 and 466 ± 85 nm for ZIF-8 and ZIF-67, respectively, comparable to those in literature using similar synthesis conditions.[17] The powder ZIF crystals appear to have both cubic and rhombic dodecahedral facets, both of which have been reported in previous studies.[30,33] ZIF-67 (NB) was found to consist of densely packed particles with an average diameter of 71 ± 12 nm and, although particles were distinct, they had no noticeable trend in shape compared to the

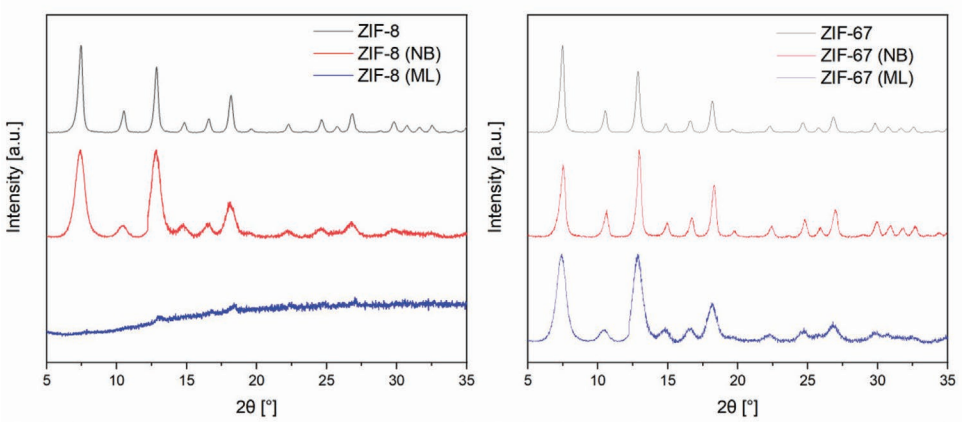

Figure 1. Powder X-ray diffraction patterns for zinc (left) and cobalt (right) ZIF samples.

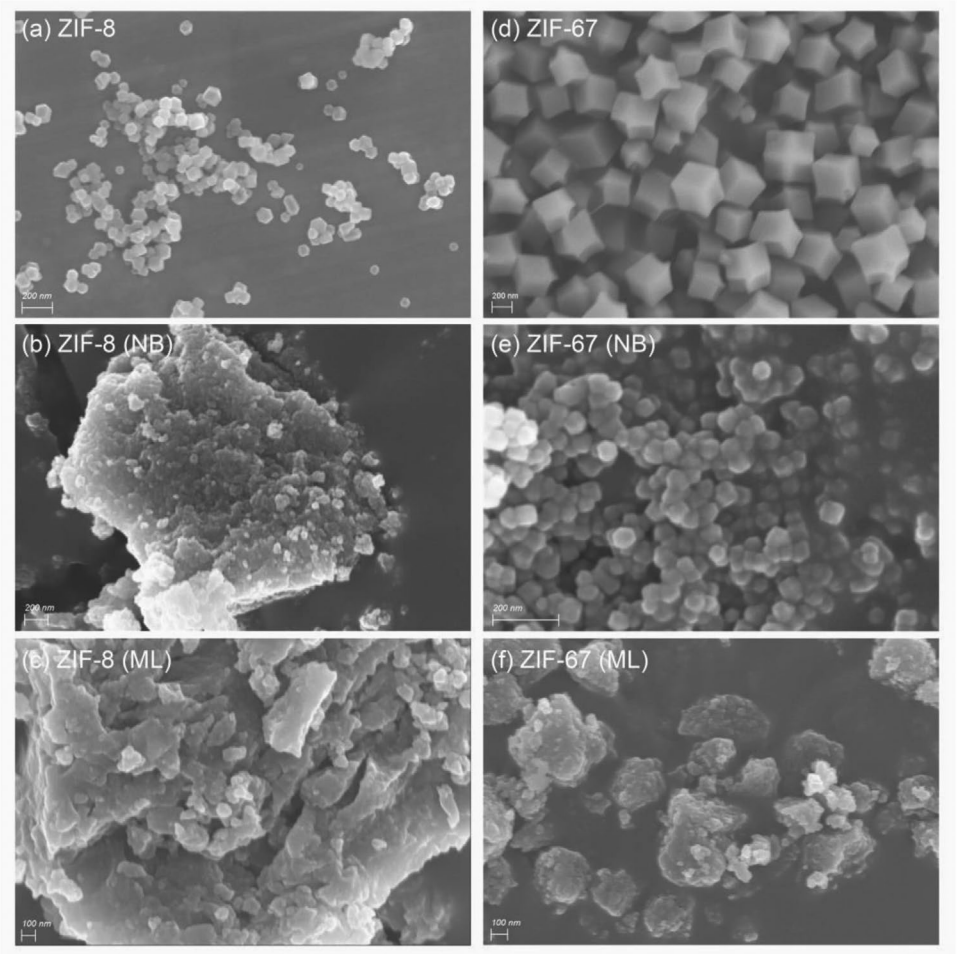

Figure 2. Scanning electron microscopy images collected for zinc (left) and cobalt (right) ZIF samples: ZIF-8, (a); ZIF-8 (NB), (b); ZIF-8 (ML), (c); ZIF-67, (d); ZIF-67 (NB), (e); and ZIF-67 (ML), (f). Scale bars for each sample shown in bottom left of image.

powder samples. Additionally, as shown in Figure 2e, many of the crystalline particles appear to be agglomerated with what is assumed to be amorphous material. ZIF-8 (NB), Z7(ML), and ZIF-67 (ML) were found to lack any distinct or well-defined particles, and crystal size distributions could not be determined.

The thermogravimetry profiles of these materials can be found in Figure S2, Supporting Information. ZIF-8 and ZIF-8 (NB) were found to be thermally stable up to temperatures of 300 °C, and lost ≈64–65% of their mass once reaching equilibrium at 1000 °C, which matches well with previous TG studies on ZIF-8.[34] ZIF-8 (ML)'s lack of crystallinity and amorphous structure conferred it ≈100 °C of additional thermal stability compared to ZIF-8, with mass loss events at 600, 800, and 1000 °C. ZIF-67 and ZIF-67 (NB) also appeared to be stable up to 300 °C, although the latter was found to have a much steeper drop in mass. ZIF-67 (ML) exhibited a mass loss of 17% below 200 °C, which is hypothesized to be due to loss of trapped unreacted 1-methylimidazole. The lack of noticeable mass loss for this temperature range in ZIF-67 (NB) implies that residual *n*-butylamine is insufficient to contribute to the mass loss of the studied monolithic ZIF-67 samples. The final mass loss of ZIF-67, ZIF-67 (NB), and ZIF-67 (ML) was found to be 64%, 66%, and 69%, respectively, at 1000 °C.

The density of ZIF-8 and ZIF-67 was measured to be 0.96 and 0.94 g cm^{-3}, respectively, which match well with literature values for ZIF-8[35] and ZIF-67[36] powders. ZIF-8 (NB) and ZIF-8 (ML) had densities of 1.17 and 1.25 g cm^{-3}, or an increase of 22% and 30% over ZIF-8, respectively. Similarly, ZIF-67 (NB) and ZIF-67 (ML) had densities of 1.11 and 1.28 g cm^{-3}, or 18% and 36% higher than ZIF-67. The mixture of *n*-butylamine and 1-methylimidazole resulted in monoliths with greater bulk densities than when modulating using only *n*-butylamine for both ZIFs. These values are summarized in **Table 1**.

Based on nitrogen adsorption data, ZIF-8 and ZIF-67 were found to have similar surface areas of 1801 and 1753 m^2 g^{-1}, respectively, although the latter was found to have greater microporosity and total pore volume. Monolithic samples prepared using single or mixed modulating ligands were found to have significantly lower surface areas than their powder counterparts, with the exception of ZIF-67 (NB) which possessed a surface area of 1732 m^2 g^{-1} (around 99% that of the powder sample). In all cases, the porosity distributions of the monolithic samples were found to differ greatly from their powdered forms. As shown in **Figure 3**, both ZIF-8 (NB) and ZIF-67 (NB) were found to have hierarchical porosity and showed an increased isotherm gradient in the P/P_0 = 0.1–0.8 region, which has been

Table 1. Physical characteristics of ZIF samples. Surface areas and porosities expressed in mass-relative and volume-relative terms. $T_{pycometry}$ = 25 °C, $T_{gas\ adsorption}$ = −196 °C.

Adsorbent	Density [g cm^{-3}]	BET surface area		Micropore volume		Total pore volume	
		[m^2 g^{-1}]	[m^2 cm^{-3}][a)]	[cm^3 g^{-1}]	[cm^3 cm^{-3}][a)]	[cm^3 g^{-1}]	[cm^3 cm^{-3}][a)]
ZIF-8	0.96	1801	1765	0.506	0.496	1.665	1.632
ZIF-8 (NB)	1.17	1597	1869	0.334	0.390	1.177	1.377
ZIF-8 (ML)	1.25	9	11	–[b)]	–[b)]	0.004	0.005
ZIF-67	0.94	1753	1648	0.583	0.548	1.779	1.672
ZIF-67 (NB)	1.11	1731	1922	0.391	0.434	1.647	1.828
ZIF-67 (ML)	1.28	1458	1866	0.515	0.660	0.643	0.823

[a)]Volume-relative quantities calculated by multiplying density by mass-relative quantity; [b)]Due to lack of micropores within sample, micropore volume could not be determined.

observed previously for ZIF-8 powders synthesized in the presence of *n*-butylamine,[30] whereas ZIF-8 and ZIF-67 were found to plateau in uptake following micropore filling. This hierarchical porosity may be due to the introduction of interstitial voids between the primary particles,[27] leading to a network of heterogeneously sized apertures. ZIF-67 (ML) was found to be predominantly microporous, lacking the increase in adsorption at the highest partial pressures, with around 80% of its pore volume being found in apertures 2 nm or less in diameter. This suggests that a mixture of *n*-butylamine and 1-methylimidazole may lead to minimal formation of inter-particle space, or that alternative drying conditions are required to form these spaces in this material. All porous samples were found to have similar sized apertures, around 0.9 and 1.7 nm for small and large pores, respectively, as shown by the calculated pore size distributions in Figure S3, Supporting Information. ZIF-8 (ML) was the only sample studied that was found to be functionally nonporous, with measured surface area and total pore volume of only 9 m^2 g^{-1} and 0.004 cm^3 g^{-1}. The higher density of the monolithic samples is reflected in their volume-relative surface areas which, apart from ZIF-8 (ML), exceeded their powder counterparts. ZIF-8 (NB), ZIF-67 (NB), and ZIF-67 (ML) were all found to have similar volumetric surface areas in the range of 1850–1950 m^2 cm^{-3}. ZIF-67 (ML) and ZIF-67 (NB) were found to have the highest volumetric micropore volume and total pore volume, at 0.660 cm^3 cm^{-3} and 1.828 cm^3 cm^{-3}, respectively.

Vapor adsorption isotherms for the 6 studied materials are shown in **Figure 4**. All samples were found to have high adsorption hydrophobicity based on their low water vapor uptake, best described as Type III isotherms.[37] ZIF-8 and ZIF-67 were found to only adsorb 23 and 39 mg g^{-1} of water vapor at P/P_0 = 0.9, noticeably higher than literature values,[6,38] although this difference is ascribed to this study's samples having a greater quantity of free space within mesopores. Monolithic samples, with the exception of ZIF-8 (ML), were all found to have higher water uptake than their powder counterparts, with capacities between 48 and 84 mg g^{-1} at the highest studied partial pressure of P/P_0 = 0.9. This suggests that monolithic ZIF samples here differ slightly in their water adsorption behavior compared to powders, perhaps due to the former's amorphous content contributing toward surface chemistry and increased mesoporosity. Typical hydrophobic industrial adsorbents studied previously,[16] activated charcoal and zeolite Y, were found to adsorb 297 and 122 mg g^{-1} of water vapor at a partial pressure of 0.8 (80% relative humidity), emphasizing the adsorption hydrophobicity of the MOFs in this work. The adsorption of toluene appeared to follow the same trend as nitrogen adsorption. At a toluene partial pressure of P/P_0 = 0.005, ZIF-8 and ZIF-67 adsorbed quantities

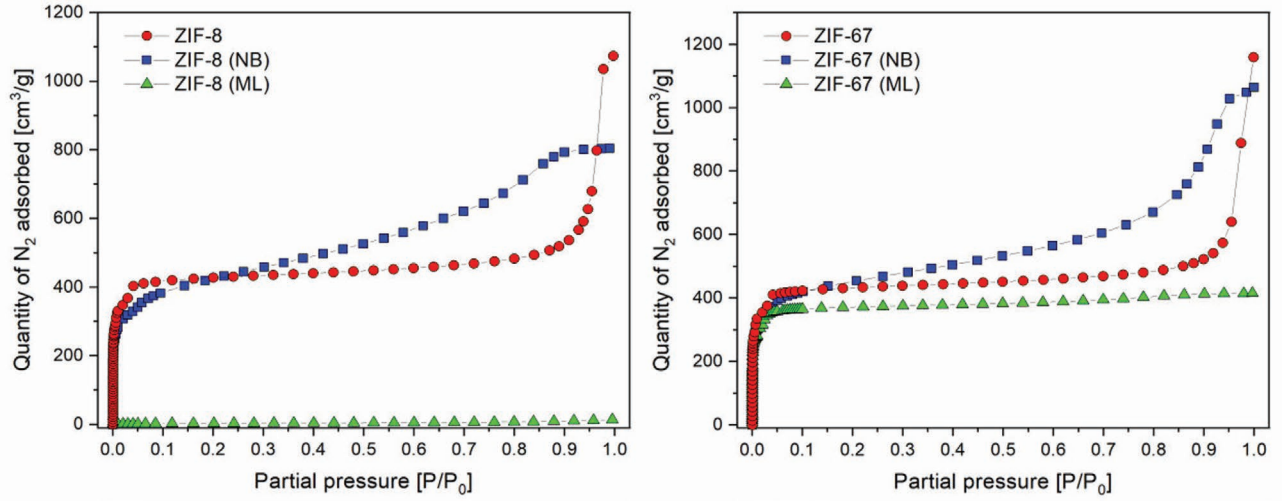

Figure 3. Nitrogen adsorption isotherms for zinc (left) and cobalt (right) ZIF samples, carried out at low temperature (–196 °C).

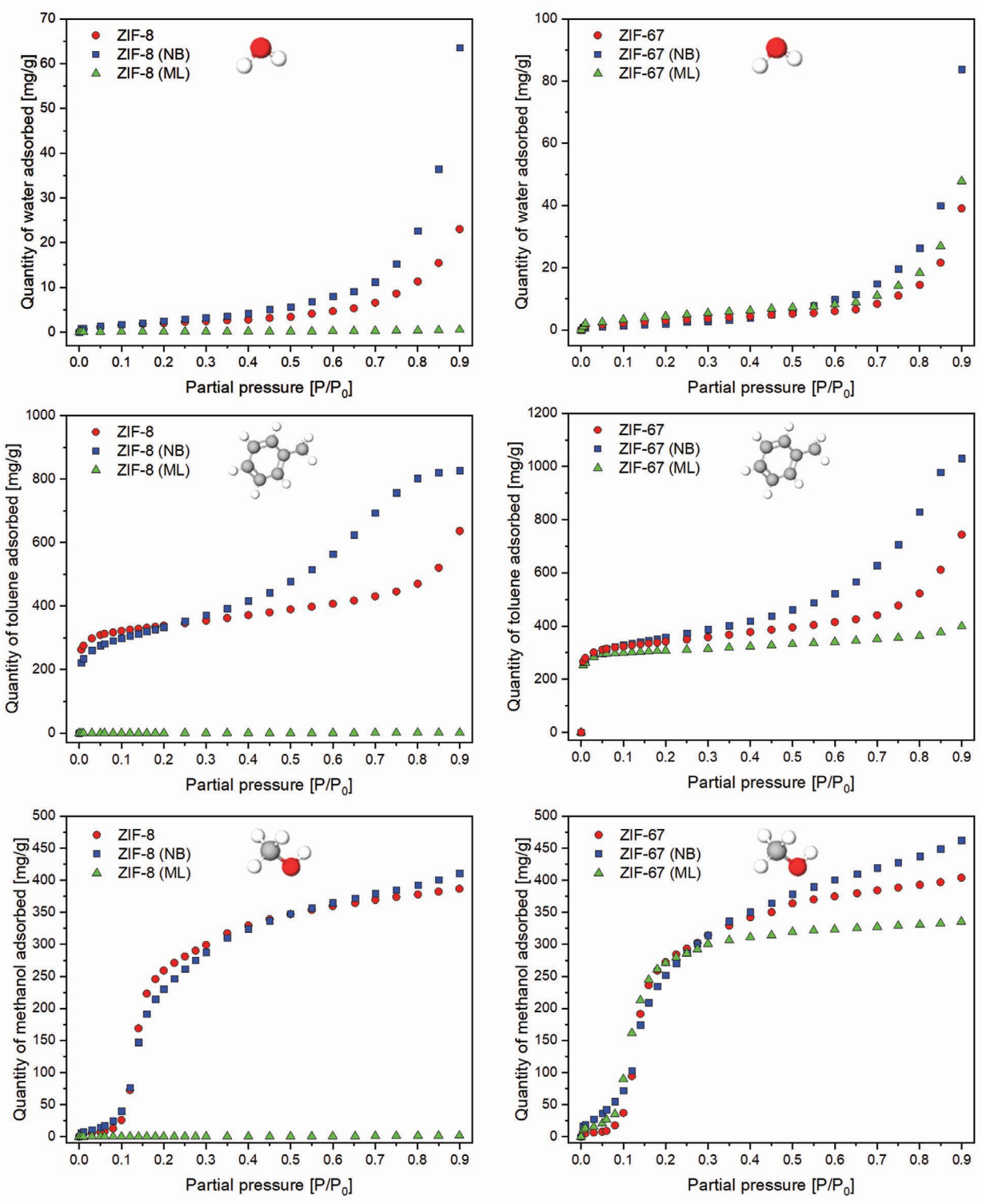

Figure 4. Vapor adsorption isotherms for zinc (left) and cobalt (right) ZIF samples. From top to bottom, vapors studied are water, toluene, and methanol. All measurements carried out at 25 °C.

of 263 and 267 mg g^{-1}, respectively, equaling that of activated charcoal (264 mg g^{-1}) in previous work.[16] While powdered samples had the greatest uptake of toluene at the lowest studied concentrations due to their higher surface areas, their uptakes plateaued afterward, resembling Type I isotherms,[37] and only noticeably increased at the highest concentrations. ZIF-8 (NB) and ZIF-67 (NB), due to their hierarchical pore structure, do not possess this flat plateau region and adsorb greater quantities

Table 2. Summary of adsorption and surface hydrophobicity of ZIF samples. Water capacity and H.I. values are quoted for medium (0.5) and high (0.9) water partial pressures. All measurements carried out at 25 °C.

Adsorbent	Water vapor capacity [mg g^{-1}]		Hydrophobicity index[a)] [mol mol^{-1}]		Advancing contact angle [°]
	$P/P_0 = 0.5$	$P/P_0 = 0.9$	$P/P_0 = 0.5$	$P/P_0 = 0.9$	
ZIF-8	3.4	23.0	15.17	2.23	112.6
ZIF-8 (NB)	5.6	63.5	7.74	0.68	124.0
ZIF-8 (ML)	0.2	0.5	0.05	0.02	131.7
ZIF-67	5.2	39.1	10.07	1.34	114.8
ZIF-67 (NB)	5.7	83.8	8.95	0.61	123.3
ZIF-67 (ML)	7.2	47.9	6.83	1.03	122.0

[a)]Calculated as molar capacity for toluene vapor at $P/P_0 = 0.005$ divided by molar capacity of water vapor at different partial pressure values.

of toluene vapor in the P/P_0 = 0.2–0.9 region, with their isotherm shapes more closely described by Type II or Type IV.[37] ZIF-8 (NB) and ZIF-67 (NB) adsorbed 826.3 and 1030.9 mg g^{-1} of toluene vapor at the highest partial pressure studied, outperforming their powder counterparts by 29.8% and 38.6%, respectively. When expressed in volume-relative terms, considering the materials' densities, ZIF-8 and -67 monoliths outperform their powder forms by 58.2% and 63.6%, respectively, further emphasizing their application in vapor adsorption. ZIF-8 (ML) had no noticeable uptake of any VOCs or water vapor, similar to nitrogen experiments. The adsorption of methanol vapor was best described by Type V isotherms for all porous samples studied. All porous samples appeared to have an inflection point around P/P_0 = 0.1, after which cage-filling occurred. This effect has been observed previously when adsorbing alcohol molecules on both hydrophobic zeolites,[16,39] as well as ZIF-8 powders.[6] Monolithic samples adsorbed greater quantities of methanol pre-inflection despite their lower surface area, suggesting that the amorphous content in these samples affects their affinity toward polar molecules.

Molar hydrophobicity indexes (H.I.s), using methods described in previous work,[16] were calculated using the adsorbed quantity of toluene at a partial pressure of 0.005, as a function of water partial pressure. A summary of these results can be found in **Table 2**, alongside contact angle and water adsorption data. Hydrophobic adsorbents from previous work were included in these plots to compare the ZIF samples in this study to standard industrial materials. All porous ZIF samples in this study were found to possess higher H.I. values than the industrial adsorbents at the highest water partial pressures studied, as shown in **Figure 5**.

Cosorption measurements found that all porous ZIF powders and monoliths were capable of adsorbing high quantities of toluene, even at water partial pressures of 0.8 (i.e., 80% relative humidity), with performances all exceeding 75% of those under dry conditions. Monolithic sample ZIF-67 (ML) and was found to possess the highest volume-relative toluene capacity under dry conditions of 322 mg cm^{-3} significantly exceeding the capacities of powder ZIF-8 and ZIF-67, both of which had capacities in the range of 250–252 mg cm^{-3}. This enhanced performance is present at the highest relative humidities, with ZIF-67 (ML) adsorbing 269 mg cm^{-3} of toluene following pre-exposure to a water partial pressure of 0.8. **Figure 6** shows the trend in capacity as a function of water partial pressure. All samples had the largest drop in performance when water partial pressure was increased from 0 to 0.2, as water molecules begin to occupy surface sites in the material. This result does not follow the trend of their water uptake, as the largest performance drop would be expected when the water adsorption is at its highest (i.e., at high partial pressures in the exponential region of the Type III isotherm). Similar to high-silica faujasites,[39] ZIF-8 and ZIF-67 have highly hydrophobic pore apertures, allowing ingress of toluene molecules even when surface sites may be occupied by water molecules. While the zinc-based samples had similar performances, with the loss in porosity of ZIF-8 (NB) offset by its increased density, the monolithic ZIF-67 samples were found to significantly outperform their powder equivalent at all humidities studied. These findings suggest that monolithic ZIFs, particularly ZIF-67 (ML) using a mixture of modulating ligands,

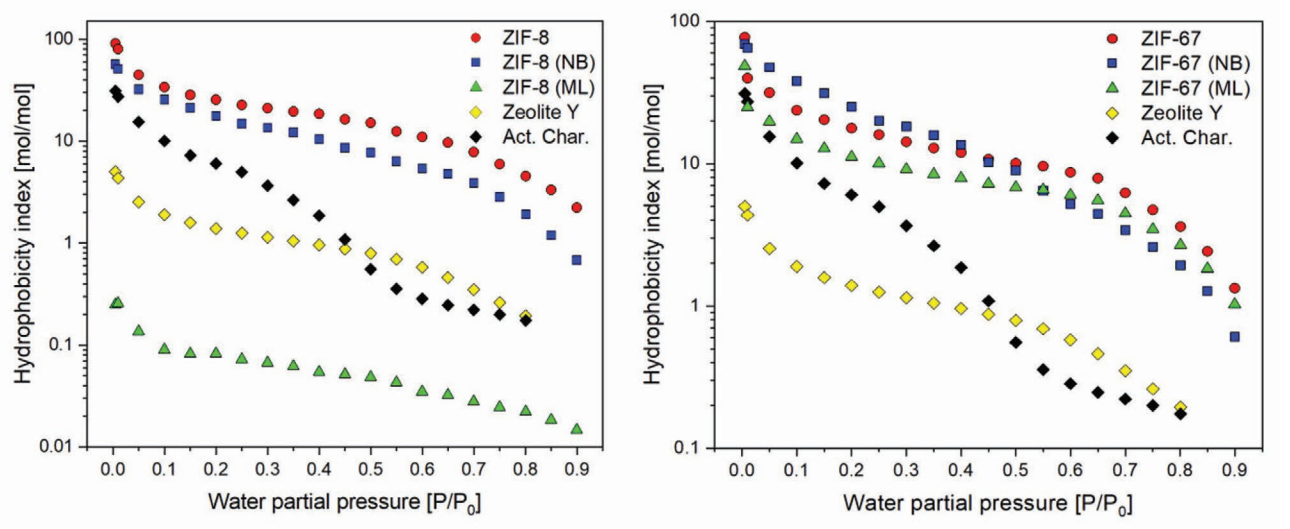

Figure 5. Hydrophobicity indexes plotted as a function of humidity, for zinc (left) and cobalt (right) ZIF samples. Plots for dealuminated zeolite Y and activated charcoal are included for comparison. All measurements carried out at 25 °C.

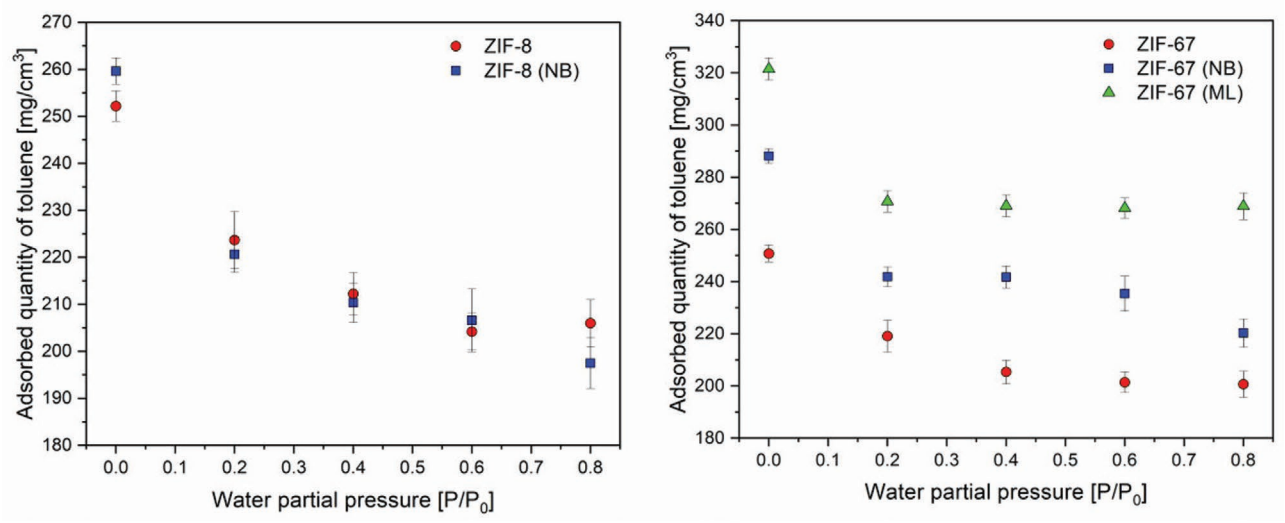

Figure 6. Cosorption volume-relative toluene vapor capacities as a function of process humidity, for zinc (left) and cobalt (right) ZIF samples. Partial pressure of toluene in all measurements, $P/P_0 = 0.005$, while water vapor partial pressure varied. All measurements carried out at 25 °C.

may be a suitable adsorbent for VOC applications in humid conditions. Not only does this sample's high density improve its efficiency for smaller-scale filters with limited operating volume, but little hydrophobicity is lost when forming the monolith, allowing it to perform well even in challenging environments.

All ZIF samples were found to have advancing contact angles above 90 °, qualifying their surface as "hydrophobic,"[40] compared to the measured contact angle of 37 ° for activated charcoal powder as seen in **Figure 7**. Monolithic samples were found to have contact angles above those of their powder equivalents. However, based on the monoliths' comparatively higher water vapor uptake their increased contact angle is possibly due to a combination of surface chemistry and surface morphology. The hydrophobicity of ZIF-8 has been demonstrated in previous studies for powder samples,[6] but never before in monoliths.

The vapor adsorption and contact angle data in this study suggests that despite the amorphous content present after synthesis via ligand- assisted methods, ZIF-8 and ZIF-67 monoliths retain their selectivity for non-polar adsorbents, while also possessing superior density. With comparable hydrophobicity to activated charcoal, as well as higher volume-relative VOC adsorption capacity under humid conditions, monolithic ZIF adsorbents could provide an effective alternative for air cleaning applications where water vapor is an important consideration.

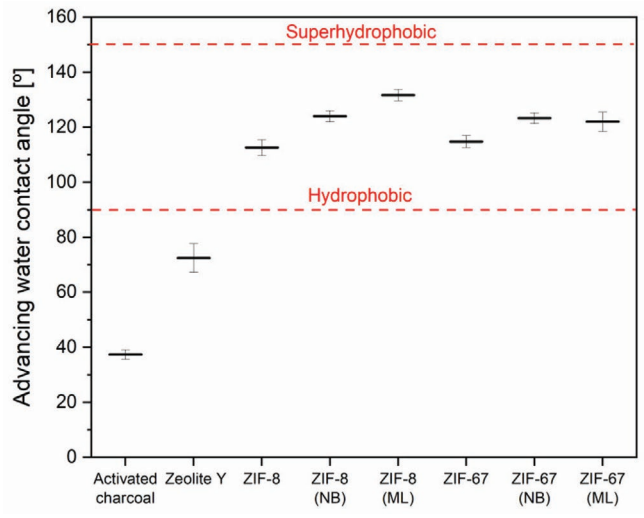

Figure 7. Summary of advancing contact angles measured for ZIF samples and activated charcoal powder.

2.1. Dynamic Toluene Adsorption

Breakthrough curves of toluene vapor at a concentration of 10 ppmv (P/P_0 = 0.00026) for the 5 studied absorbents are shown in **Figure 8**, the results of which are summarized in **Table 3**. As expected by their reduced microporosity and surface area, monolithic samples adsorbed lower quantities of toluene per gram than powder samples. However, when breakthrough curves and capacities are normalized by volume, every monolithic sample either matched or outperformed their powder counterpart, by up to 34%. ZIF-67 (ML) was found to have the highest capacity, similar to the results in the gravimetric toluene tests, due to its superior volumetric micropore volume, and high volumetric surface area. Adsorbent beds consisting of monolithic samples exhibited negligible pressure drops (<0.01 bar) at gas flowrates of 50 and 100 mL min^{-1}, while powdered ZIF-8 and ZIF-67 columns exhibited pressure drops at these flowrates in the range of 0.26–0.27 and 0.51–0.54 bar, respectively. Fine powders, such as activated charcoal, were tested and exhibited pressure drops 3 times that of the ZIF powders, exceeding the safe operating conditions of the column at 100 mL min^{-1}. Granular adsorbents, such as molecular sieve 13X and zeolite Y exhibited similarly very low pressure drops to ZIF monoliths, all below 0.04 bar. For applications at higher gas velocities, packed beds of powders will exhibit greater pressure drops and may result in reductions in efficiency or bed collapse. The structured adsorbents in this study avoid this issue, with minimal loss in performance compared to their equivalent powders.

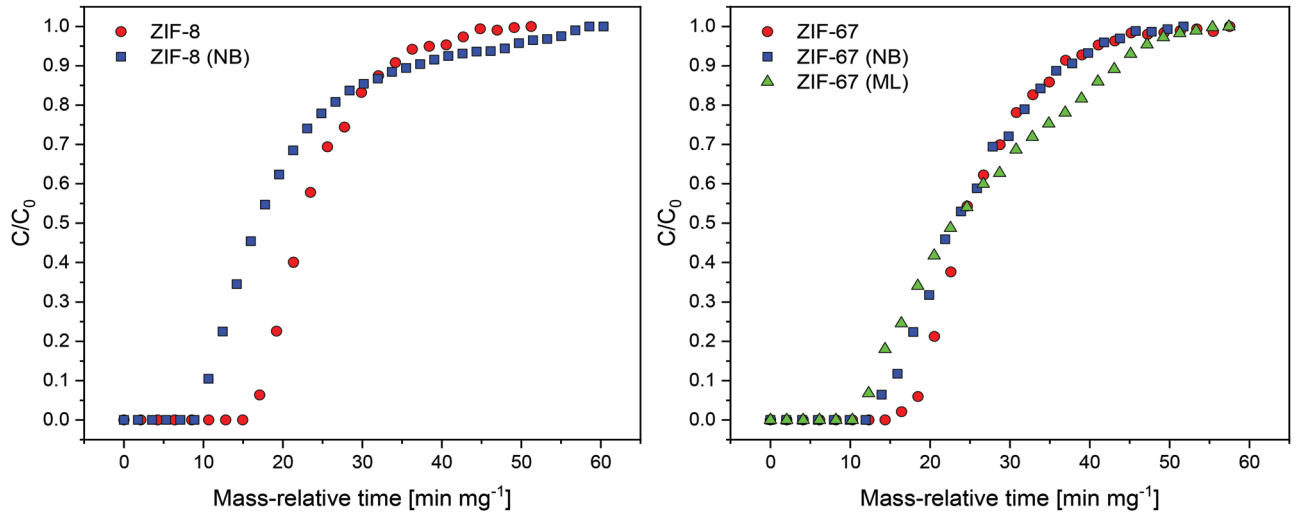

Figure 8. Breakthrough curves of toluene vapor on zinc- (left) and cobalt- (right) based adsorbents. Time axis has been made relative to sample mass for clarity. All measurements carried out at toluene partial pressure of 0.00026, and a temperature of 25 °C.

Due to the low concentration driving force, the kinetics for toluene adsorption at these concentration levels is slow, as shown by the low gradient following vapor breakthrough. This resulted in low percentage usability, calculated as the ratio of capacity before breakthrough and the total capacity after the column is completely saturated. The highest usability measured was for ZIF-8 powder, at 60.1%. This reduced effectiveness from low driving force is exacerbated in ZIF-8 and ZIF-67, due to their pore flexibility under gas intrusion.[41]

2.2. Toluene Adsorption Productivities

The estimated productivities for toluene adsorption on a mass- and volume- relative basis are shown in **Table 4**. Per kilogram, ZIF-67 (NB) was found to have the highest productivity, due to its high capacity in intermediate pressure ranges, as well as having the shortest adsorption timeframe. ZIF-67 (NB) was then followed by the two powdered ZIFs which had higher mass-relative productivities than two of their monolith counterparts ZIF-67 (ML) and ZIF-8 (NB). However, when density was considered, ZIF-67 (NB) still had the highest productivity of 81.3 kg of toluene adsorbed per cubic meter of adsorbent per hour, 27% higher than its powder counterpart, followed by the other monolithic adsorbents. The final choice between powdered or structured adsorbents will depend on the limiting factor of the filtration process, that is, sample mass or available filter unit volume, though in many operational industrial scenarios, volumetric performance will be of high importance.

Table 3. Summary of low concentration dynamic adsorption experiments. All measurements carried out at a toluene partial pressure of 0.00026, and a temperature of 25 °C.

Adsorbent	Capacity [mg g^{-1}]		Capacity [mg cm^{-3}]		Usability [%][a]
	Useable	Total	Useable	Total	
ZIF-8	56.3	93.7	54	90	60.1
ZIF-8 (NB)	34.3	76.8	40.2	89.8	44.7
ZIF-67	54.4	97.2	51.2	91.4	56
ZIF-67 (NB)	44.7	92.1	49.6	102.3	48.5
ZIF-67 (ML)	39.4	95.9	50.5	122.8	41.1

[a]Calculated by dividing capacity when toluene is first detected by the capacity when the inlet and outlet concentrations of toluene are equal.

3. Conclusions

In summary, the synthesis of monolithic ZIF-8 and ZIF-67 was carried out using solvothermal methods under room temperature and pressure. The choice of modulating ligand appeared to be the key in determining the crystallinity of the final product, as well as its porosity and surface area. All samples synthesized using modulators were found to have reduced crystallinity based on diffraction and microscopy measurements. Despite this, all samples except ZIF-8 (ML) were found to have high porosities which, when assessed in volume-relative terms, exceeded those of their powder equivalents due to increased density. The addition of *n*-butylamine as a modulating ligand appeared to produce hierarchical porosity into both ZIF-8 and ZIF-67 samples, while a mixture of 1-methylimidazole and *n*-butylamine produced ZIF-67 with predominantly microporous structure. Contact

Table 4. Estimated mass-relative and volume-relative toluene vapor capture productivities for adsorbents. Calculated using gravimetric toluene adsorption data at a partial pressure of 0.1 and a temperature of 25 °C.

Sample	Capacity [mg g^{-1}]	Time [min][a]	Productivity	
			[kg (kg h)$^{-1}$]	[kg (m^3 h)$^{-1}$]
ZIF-8	321.8	274	0.0705	67.9
ZIF-8 (NB)	298.6	293	0.0611	71.5
ZIF-67	323.9	285	0.0682	64.1
ZIF-67 (NB)	329.4	270	0.0732	81.3
ZIF-67 (ML)	299.7	300	0.0599	76.7

[a]Time taken to reach a mass gradient value of 0.00075 % dry mass per minute.

angle and vapor adsorption measurements found that while the monoliths exhibited higher surface hydrophobicity, their amorphous content led to an increase in their affinity for water and methanol vapor. All porous samples had high capacities for toluene vapor, even at partial pressures of $P/P_0 \approx 0.00026$, meaning the monolithic samples retained the flexibility of the ZIF apertures. These hydrophobic ZIFs produced toluene adsorption levels higher than traditional industrial adsorbents, and adsorbed smaller quantities of water vapor at the highest humidity values studied. Cosorption measurements found that all porous samples studied were able to adsorb high quantities of toluene vapor even at water partial pressures of 0.8. Based on the ligands chosen, monoliths were found to excel in different adsorption applications: Single-modulator monoliths excelled at adsorbing toluene at high partial pressures, exceeding their powder counterparts by over 50%; ZIF-67 mixed-modulator monoliths were able to adsorb the highest quantities of toluene under low-concentration, high humidity conditions. Finally, the reduction in packed bed pressure drop from monolithic samples emphasis their potential function in dynamic adsorption processes such as column filtration or recovery. The ability to tune the properties of monolithic ZIFs, synthesized under ambient conditions via sol–gel formation, by altering the choice of modulating caps used could provide an advancement in the applicability of future framework materials for organic vapor capture under real-world conditions

4. Experimental Section

Materials: All reactants for synthesis were ordered with a minimum of 99% purity: Zinc nitrate hexahydrate, cobalt nitrate hexahydrate, and 2-methylimidazole were ordered from Sigma-Aldrich (USA); modulating ligands *n*-butylamine and 1-methylimidazole were ordered from Sigma-Aldrich (USA); and methanol was ordered from VWR International (USA). For the generation of vapor isotherms the same supplier of methanol was used, toluene was ordered from Thermo Fischer Scientific (USA), and in-house deionized water was used for water vapor and contact angle measurements. Activated charcoal powder was acquired from Sigma-Aldrich (USA).

Synthesis of Powder Adsorbents: For the synthesis of ZIF-8 and ZIF-67 powders, 0.745 g (≈2.5 mmol) of zinc nitrate hexahydrate or 0.720 g (≈2.5 mmol) of cobalt nitrate hexahydrate, respectively, was dissolved in 50 mL of methanol. A second solution was prepared by dissolving 1.642 g (≈20 mmol) of 2-methylimidazole in 50 mL of methanol, which was combined with the first solution under magnetic bar stirring until solutions were well mixed. After 24 h the resulting precipitate was centrifuged and washed with methanol 3 times before drying under vacuum at room temperature overnight. ZIF-8 and ZIF-67 powders prepared in this way were denoted as ZIF-8 and ZIF-67, respectively.

Synthesis of Monolithic Adsorbents Using Single Modulating Ligand: The monolithic samples were prepared almost identically to the powders, apart from the addition of 1.98 mL (≈20 mmol) of *n*-butylamine to the solution containing 2-methylimidazole. In addition, the cleaned sol–gel product was allowed to air dry under ambient temperature and pressure (i.e., instead of vacuum drying) for a period of 72 h, producing monoliths on the scale of a few millimeters. These samples were denoted as ZIF-8 (NB) and ZIF-67 (NB) for ZIF-8 and ZIF-67, respectively.

Synthesis of Monolithic Adsorbents Using Multiple Modulating Ligands: To test the effects of a mixture of modulating ligands on monolith formation, a mixture of 0.797 mL (≈10 mmol) of 1-methylimidazole and 0.985 mL (≈10 mmol) of *n*-butylamine was added to the solution containing 2-methylimidazole. The precipitates were then treated in an identical manner to the previous procedure. These samples prepared using mixed ligands were denoted as ZIF-8 (ML) and ZIF-67 (ML) for ZIF-8 and -67, respectively.

Physical Characterization of Adsorbents: Powder X-ray diffraction patterns were collected using an X'Pert Pro X-ray diffractometer (Malvern Panalytical, UK) with the following operating conditions: Cu-Kα radiation at 40 kV and 20 mA, in a 2θ scan range of 4°–60°, using a step size of 0.03°. Relative crystallinity was determined by integrating the baseline-adjusted crystalline peaks at 2θ values up to 18.1°, and comparing to the same-metal sample with the highest area. Thermogravimetry profiles were determined using an STA 449 F5 Jupiter (NETZSCH, Germany). Sample temperatures were raised from 50 to 1000 °C at a rate of 5 °C min^{-1} using a carrier gas of dry air. The density of adsorbent samples was measured via pycnometry using an Accupyc II 1340 (Micromeritics, USA), with Helium gas as the probe molecule. All density measurements were carried out at room temperature, $T = 25$ °C.

Surface area, pore volume, and pore size distributions were determined via nitrogen sorption, measured at –196 °C using a 3-Flex Physisorption (Micromeritics, USA). Before analysis, samples were activated overnight at 200 °C under vacuum, and 150 °C using the equipment's in situ vacuum activation in order to completely remove any water or contaminants present. Brunauer–Emmett–Teller surface area values were determined using data points in the partial pressure region of $P/P_0 = 0.02$–0.08. Micropore and total pore volumes were determined using the t-plot and single-point volume adsorbed methods, respectively. Pore size distributions were determined from adsorption data using non-linear density functional theory models, assuming cylindrical pore geometry.

Adsorption and Surface Hydrophobicity of Adsorbents: Adsorption isotherms for water, toluene, and methanol vapor were collected gravimetrically using a DVS Endeavour (Surface Measurement Systems, UK). Concentrations were generated using liquid solvent bubbling reservoirs and controlled via closed-loop speed of sound sensors. Prior to each experiment, 20–50 mg of sample was activated at 200 °C under vacuum for 4 h to remove any residual moisture or other contaminants that may influence adsorption performance. Cosorption measurements were carried out using the dual-solvent move of the DVS Endeavour. Following activation, samples were exposed to a certain partial pressure of water vapor and, while this pressure was maintained, a step increase in toluene concentration of $P/P_0 = 0.005$ was introduced to measure the uptake of toluene vapor under humid conditions.

Surface hydrophobicity was estimated using advancing contact angle measurements, carried out using a Krüss DSA25 (Krüss Scientific, Germany). Each sample was ground to a fine powder before being attached to a flat glass slide via double-sided adhesive tape. Contact angles were measured for progressively larger water droplet volumes until the angle decreased, with the advancing contact angle being the one preceding this decrease. Each experiment was repeated a total of 5 times and averaged to minimize site heterogeneity. Measurements were also carried out on activated charcoal and zeolite Y powders to provide a comparison between the ZIF samples and standard adsorbents.

Dynamic Vapor Adsorption Tests: Dynamic toluene breakthrough experiments were carried out using a breakthrough analyzer built in-house. For each experiment, 4 mm I.D. borosilicate columns were packed with adsorbent, and regenerated using an in situ oven for 3 h at 120 °C prior to each measurement. Dry air was used as the carrier gas in all experiments, with a flowrate of 100 mL min^{-1}. Pressure drop measurements were carried out at several gas flowrates. VOC concentrations were measured using a photoionization detector (Ionscience, United Kingdom). For pressure drop calculations, equal bed lengths of 2 cm were packed inside columns, with pressure drop measured for gas flowrates of 50 and 100 mL min^{-1} using a digital pressure gauge (Wika, United Kingdom).

Adsorbent Productivity Estimates: The productivity of an adsorption process or column was estimated by dividing the adsorption capacity of a material by the total time elapsed during the adsorption step. Estimates were calculated under a toluene partial pressure of 0.1, using kinetic data from the DVS Endeavour. The time elapsed was defined as the time taken to reach an adsorption gradient value of 0.00075% dry mass per minute. The effect of vacuum intensity and temperature on regeneration time was not investigated in this study.

Supporting Information

Supporting Information is available from the Wiley Online Library or from the author.

Acknowledgements

This work was supported by the EPSRC Centre for Doctoral Training in Advanced Characterisation of Materials (Grant Ref: EP/L015277/1), as well as Procter & Gamble Co., USA. The authors acknowledge use of characterization facilities within the Harvey Flower Electron Microscopy Suite, Department of Materials, Imperial College London. The authors acknowledge Patricia Carry and Kaho Cheung for assisting with physical characterization experiments.

Conflict of Interest

The authors declare no conflict of interest.

Keywords

adsorption, hydrophobicity, monolith, porosity tuning, zeolitic imidazolate framework

Received: September 30, 2020
Published online:

[1] K. Noh, J. Lee, J. Kim, *Isr. J. Chem.* **2018**, *58*, 1075.
[2] S. Cao, T. D. Bennett, D. A. Keen, A. L. Goodwin, A. K. Cheetham, *Chem. Commun.* **2012**, *48*, 7805.
[3] S. Bhattacharjee, M. S. Jang, H. J. Kwon, W. S. Ahn, *Catal. Surv. Asia* **2014**, *18*, 101.
[4] A. Phan, C. J. Doonan, F. J. Uribe-Romo, C. B. Knobler, M. O'Keeffe, O. M. Yaghi, *Acc. Chem. Res.* **2010**, *43*, 58.
[5] W. Ma, Q. Jiang, P. Yu, L. Yang, L. Mao, *Anal. Chem.* **2013**, *85*, 7550.
[6] K. Zhang, R. P. Lively, C. Zhang, R. R. Chance, W. J. Koros, D. S. Sholl, S. Nair, *J. Phys. Chem. Lett.* **2013**, *4*, 3618.
[7] M. Tu, S. Wannapaiboon, K. Khaletskaya, R. A. Fischer, *Adv. Funct. Mater.* **2015**, *25*, 4470.
[8] R. Wei, H. Y. Chi, X. Li, D. Lu, Y. Wan, C. W. Yang, Z. Lai, *Adv. Funct. Mater.* **2020**, *30*, 1.
[9] D. Kim, D. W. Kim, O. Buyukcakir, M. K. Kim, K. Polychronopoulou, A. Coskun, *Adv. Funct. Mater.* **2017**, *27*, 1.
[10] Y. Feng, Y. Li, M. Xu, S. Liu, J. Yao, *RSC Adv.* **2016**, *6*, 109608.
[11] S. Zhan, Z. Gao, F. Xia, E. E. Sann, Y. Pan, *Sep. Purif. Technol.* **2018**, *206*, 186.
[12] S. Jafari, F. Ghorbani-Shahna, A. Bahrami, H. Kazemian, *Appl. Sci.* **2018**, *8*, 310.
[13] F. Chu, Y. Zheng, B. Wen, L. Zhou, J. Yan, Y. Chen, *RSC Adv.* **2018**, *8*, 2426.
[14] P. Wolkoff, G. D. Nielsen, *Environ. Int.* **2017**, *101*, 96.
[15] H. Nigar, N. Navascués, O. De La Iglesia, R. Mallada, J. Santamaría, *Sep. Purif. Technol.* **2015**, *151*, 193.
[16] E. Hunter-Sellars, J. J. Tee, I. P. Parkin, D. R. Williams, *Microporous Mesoporous Mater.* **2020**, *298*, 110090.
[17] K. Zhou, B. Mousavi, Z. Luo, S. Phatanasri, S. Chaemchuen, F. Verpoort, *J. Mater. Chem. A* **2017**, *5*, 952.
[18] A. Elsayed, S. Mahmoud, R. Al-Dadah, J. Bowen, W. Kaialy, *Energy Procedia* **2014**, *61*, 2327.
[19] F. Akhtar, L. Andersson, S. Ogunwumi, N. Hedin, L. Bergström, *J. Eur. Ceram. Soc.* **2014**, *34*, 1643.
[20] T. Tian, J. Velazquez-Garcia, T. D. Bennett, D. Fairen-Jimenez, *J. Mater. Chem. A* **2015**, *3*, 2999.
[21] J. P. Mehta, T. Tian, Z. Zeng, G. Divitini, B. M. Connolly, P. A. Midgley, J. C. Tan, D. Fairen-Jimenez, A. E. H. Wheatley, *Adv. Funct. Mater.* **2018**, *28*, 1705588.
[22] R. N. Widmer, G. I. Lampronti, B. Kunz, C. Battaglia, J. H. Shepherd, S. A. T. Redfern, T. D. Bennett, *ACS Appl. Nano Mater.* **2018**, *1*, 497.
[23] S. E. Bambalaza, H. W. Langmi, R. Mokaya, N. M. Musyoka, J. Ren, L. E. Khotseng, *J. Mater. Chem. A* **2018**, *6*, 23569.
[24] R. V. Jasra, B. Tyagi, Y. M. Badheka, V. N. Choudary, T. S. G. Bhat, *Ind. Eng. Chem. Res.* **2003**, *42*, 3263.
[25] J. Hou, A. F. Sapnik, T. D. Bennett, *Chem. Sci.* **2020**, *11*, 310.
[26] T. Tian, Z. Zeng, D. Vulpe, M. E. Casco, G. Divitini, P. A. Midgley, J. Silvestre-Albero, J. C. Tan, P. Z. Moghadam, D. Fairen-Jimenez, *Nat. Mater.* **2018**, *17*, 174.
[27] B. M. Connolly, M. Aragones-Anglada, J. Gandara-Loe, N. A. Danaf, D. C. Lamb, J. P. Mehta, D. Vulpe, S. Wuttke, J. Silvestre-Albero, P. Z. Moghadam, A. E. H. Wheatley, D. Fairen-Jimenez, *Nat. Commun.* **2019**, *10*, 1.
[28] K. Sumida, K. Liang, J. Reboul, I. A. Ibarra, S. Furukawa, P. Falcaro, *Chem. Mater.* **2017**, *29*, 2626.
[29] B. Bueken, N. V. Velthoven, T. Willhammar, T. Stassin, I. Stassen, D. A. Keen, G. V. Baron, J. F. M. Denayer, R. Ameloot, S. Bals, D. D. Vos, T. D. Bennett, *Chem. Sci.* **2017**, *8*, 3939.
[30] J. Cravillon, R. Nayuk, S. Springer, A. Feldhoff, K. Huber, M. Wiebcke, *Chem. Mater.* **2011**, *23*, 2130.
[31] C. F. Holder, R. E. Schaak, *ACS Nano* **2019**, *13*, 7359.
[32] I. H. Lim, W. Schrader, F. Schüth, *Chem. Mater.* **2015**, *27*, 3088.
[33] P. Y. Moh, M. Brenda, M. W. Anderson, M. P. Attfield, *CrystEngComm* **2013**, *15*, 9672.
[34] A. Schejn, L. Balan, V. Falk, L. Aranda, G. Medjahdi, R. Schneider, *CrystEngComm* **2014**, *16*, 4493.
[35] J. C. Tan, T. D. Bennett, A. K. Cheetham, *Proc. Natl. Acad. Sci. USA* **2010**, *107*, 9938.
[36] A. Khan, M. Ali, A. Ilyas, P. Naik, I. F. J. Vankelecom, M. A. Gilani, M. R. Bilad, Z. Sajjad, A. L. Khan, *Sep. Purif. Technol.* **2018**, *206*, 50.
[37] M. Thommes, K. Kaneko, A. V. Neimark, J. P. Olivier, F. Rodriguez-Reinoso, J. Rouquerol, K. S. W. Sing, *Pure Appl. Chem.* **2015**, *87*, 1051.
[38] K. Zhang, R. P. Lively, M. E. Dose, A. J. Brown, C. Zhang, J. Chung, S. Nair, W. J. Koros, R. R. Chance, *Chem. Commun.* **2013**, *49*, 3245.
[39] I. Halasz, S. Kim, B. Marcus, *J. Phys. Chem. B* **2001**, *105*, 10788.
[40] K. Y. Law, *J. Phys. Chem. Lett.* **2014**, *5*, 686.
[41] T. Ueda, T. Yamatani, M. Okumura, *J. Phys. Chem. C* **2019**, *123*, 27542.